THREE-DIMENSIONAL MODELING AND VISUALIZATION OF WHOLE NORWAY SPRUCE LATEWOOD TRACHEIDS

Stig L. Bardage

Research Scientist
Wood Ultrastructure Research Center
Swedish University of Agricultural Science
Department of Wood Science
P.O. Box 7008
SE-750 07 Uppsala, Sweden

(Received September 2000)

ABSTRACT

The three-dimensional morphology of four whole Norway spruce latewood tracheids is described in this work. Tracheids are shown to have a characteristic shape composed of five different morphological zones. Visualization of the different morphological zones was accomplished with the use of computerized three-dimensional (3D) reconstruction. 3D reconstructions were generated from stacks of micrographs obtained from serial sections of a wood block. The micrographs were processed and integrated in a CAD-based computerized modeling system using Non-Uniform Rational B-Splines (NURBS), which produces 3D reconstructions consisting of surfaces or volumetric bodies. Volumetric changes in relation to hydration state of latewood tracheid segments were studied. It was found that tracheid tips swell less than central regions, and that as a consequence of swelling, the cell walls of Norway spruce latewood tracheids expand inward towards the lumen.

Keywords: Three-dimensional, reconstruction, modeling, spruce, *Picea abies,* latewood tracheids, tracheid width, cell-wall thickness, swelling, shrinkage.

INTRODUCTION

Tracheid distribution, length, width, and cell-wall thickness of a variety of tree species have been continuously studied by many scientists (Helander 1933; Vasiljevic 1955; Bannan 1965; Fengel 1969; Panshin and de Zeeuw 1980; Atmer and Thörnqvist 1982; Sarämpää 1994; Tyrväinen 1995; Lindström 1997; Herman et al. 1998). These types of data were often derived from measurements performed on sections or macerated tissue. These measurements often show great variations and normally do not take into account longitudinal variations of tracheids or their three-dimensionality. The microstructure of tracheids is known to be important for the physical and mechanical properties of wood and wood products. It will also influence the physical and mechanical properties of pulp and paper.

Only a few attempts to produce three-dimensional (3D) reconstructions of wood structure at the microscopical level have been made so far (Lewis 1935; Suzuki et al. 1991; Fujii 1993; Fujita and Saiki 1996; Wang and Shaler 1998). In early work by Lewis (1935), serial transverse sections were used to study the arrangement and shape of pine tracheids. 3D visualization was achieved with the use of wax plate reconstructions. Suzuki et al. (1991) visualized the arrangement of wood cells in poplar by connecting their centers of gravity along a stack of images. Fujii (1993) studied the anatomy of some Japanese species of *Fragaceae* on resin casts with scanning electron microscopy. The resin casts were achieved by embedding dry wood blocks in polystyrene and completely removing cell walls through repeated treatments with peroxide/acetic acid solutions and sulfuric acid. Fujita and Saiki (1996) created a 3D reconstruction of the distribution of vessels in *Aesculus turbinata.* In a more technical oriented paper, Wang and Shaler (1998) presented computer simulations of the three-dimensional microstructure of wood fiber composite materials, although in this

Wood and Fiber Science, 33(4), 2001, pp. 627–638

study fibers were represented as rigid cylinders. 3D models are now being used more frequently in biological science to provide new perspectives into the morphological organization of biological structures and tissues (Emons and Mulder 1998; Zelling and Perktold 1998).

Wood shrinks anisotropically during drying. In coniferous wood, this phenomenon has been considered to arise mainly from the difference in shrinkage between earlywood and latewood, although it is influenced by ray tissue, microfibrillar orientation, and pit structure (Kollmann and Côté 1984). However, separated earlywood by itself has been reported to show transverse anisotropic shrinkage (Pentoney 1953; Nakato and Kajita 1955; Watanabe et al. 1998). This fact suggests that anisotropic shrinkage may also be related to cell shape and arrangement.

A methodology for computerized 3D reconstruction and visualization of wood microstructure has been developed within the Wood Ultrastructure Research Centre (WURC), Department of Wood Science, Swedish University of Agricultural Sciences, Uppsala, Sweden. 3D reconstructions are easily generated from stacks of micrographs obtained from serial sections of wood blocks. The micrographs are processed and integrated in a CAD-based computerized modeling system using Non-Uniform Rational B-Splines (NURBS) for the extraction of shapes. 3D reconstructions consisting of surfaces or volumetric bodies can be produced. The 3D models can be moved in X, Y, and Z directions allowing tilt and rotation. This allows the examination of reconstructions from different angles. Reconstructions can also be digitally sectioned and deformed and are capable of providing linear and volumetric measurement data. Norway spruce wood and pulp fibers are currently being studied using this technique. Image analysis and computerized 3D reconstruction were combined in the present work to reveal the micromorphology of whole Norway spruce latewood tracheids as a first step in the modeling of whole tracheid structure.

The objective of the present work was to study whole tracheid morphology and physical behavior in wood with the aid of computerized 3D reconstruction. This type of approach may provide a more detailed understanding of Norway spruce (*Picea abies*) wood fiber structure and properties.

MATERIALS AND METHODS

The samples used in this work came from a wood disc of Norway spruce (*Picea abies* [L.] Karst) collected at one quarter of tree stem height from a tree that was growing in the center of Sweden (Ludvika/Hällefors). The tree was 51 years old and the stem was growing with an inclination of 10°. A block (10 mm × 10 mm × 15 mm) comprising year rings 38–43 was taken from the outer part of the disc in an area free from compression wood and was prepared for serial sectioning using a sledge microtome. A total of 192 consecutive transverse sections (20 μ thick) were made without further pretreatment. The shortest unit length corresponds to 20 μm. Sections were mounted on objective glasses with water and scanned for tracheid tips with a light microscope to allow localization of a suitable area to begin image acquisition. One hundred forty-two transverse sections covered four whole tracheids belonging to one and the same radial row. Sequential images of hydrated transverse sections were acquired using a light microscope fitted with a CCD-camera attached to a computer (Pentium II). The sections were then dried at room temperature and coated with carbon prior to observations with a scanning electron microscope (JEOL JSM-5800LV). Sequential images of dried sections were taken with the scanning electron microscope (SEM) at the same position as for the hydrated samples. All images were stored and processed digitally. The four latewood tracheids studied, which derived from the same cambium mother cells, were numbered in a decreasing sequence (9, 8, 7, and 6) towards the year ring border at the latewood side. Image analysis was performed with the softwares ImagePro PLUS

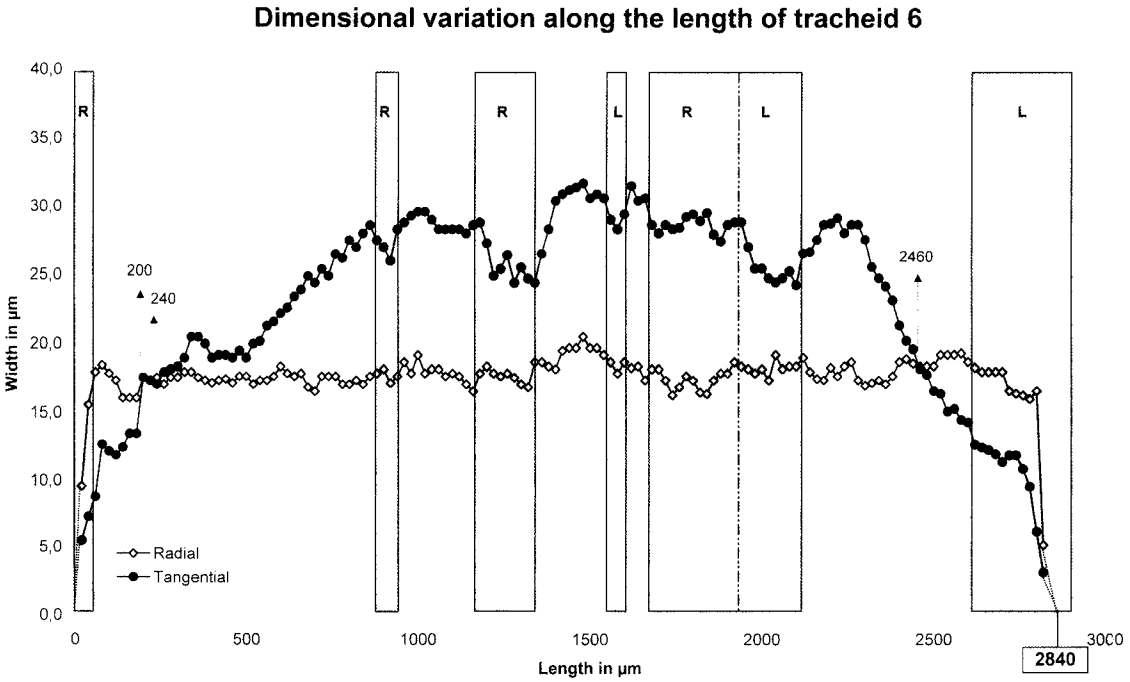

FIGS. 1–4. Variation in radial and tangential widths along the length of dried latewood tracheids. Shaded areas represent neighboring rays. R (right) and L (left) denote the position of rays seen from a tangential view.

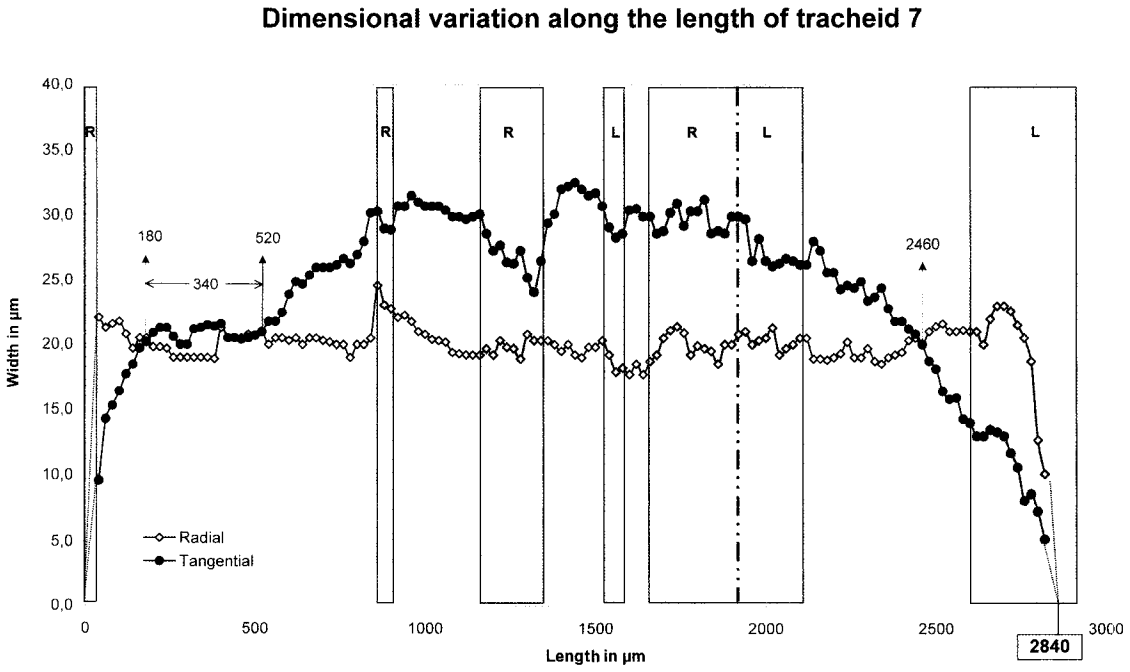

FIG. 2.

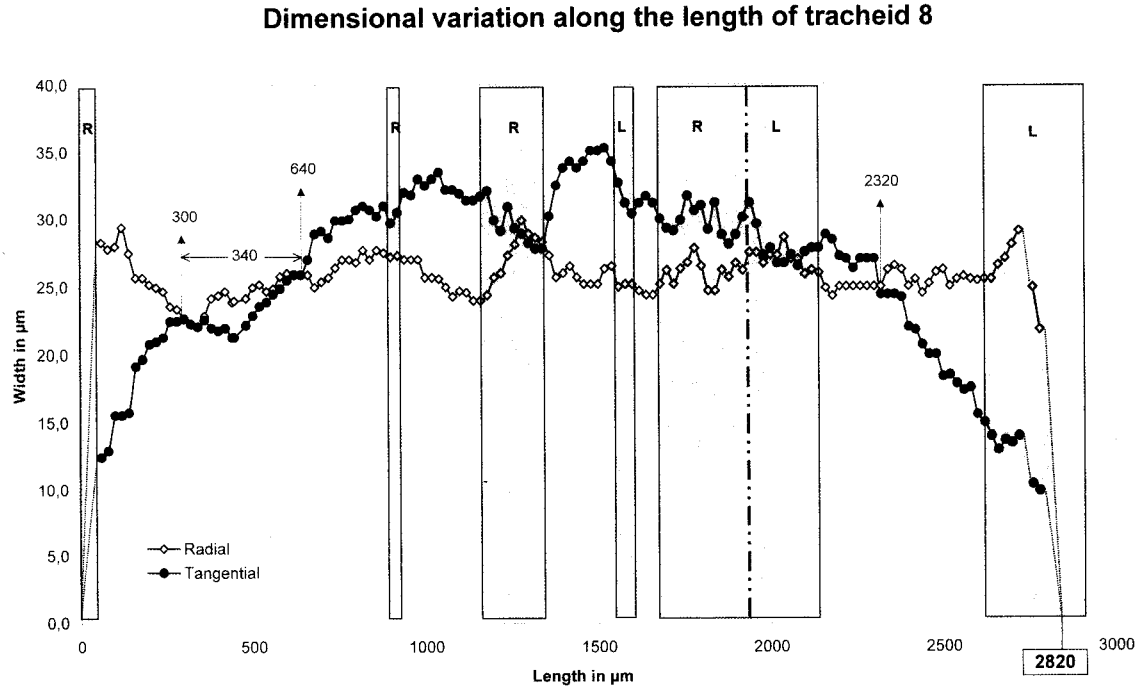
Dimensional variation along the length of tracheid 8
Width in µm
Length in µm
Radial
Tangential
R
L
300
340
640
2320
2820
0,0
5,0
10,0
15,0
20,0
25,0
30,0
35,0
40,0
0
500
1000
1500
2000
2500
3000

FIG. 3.

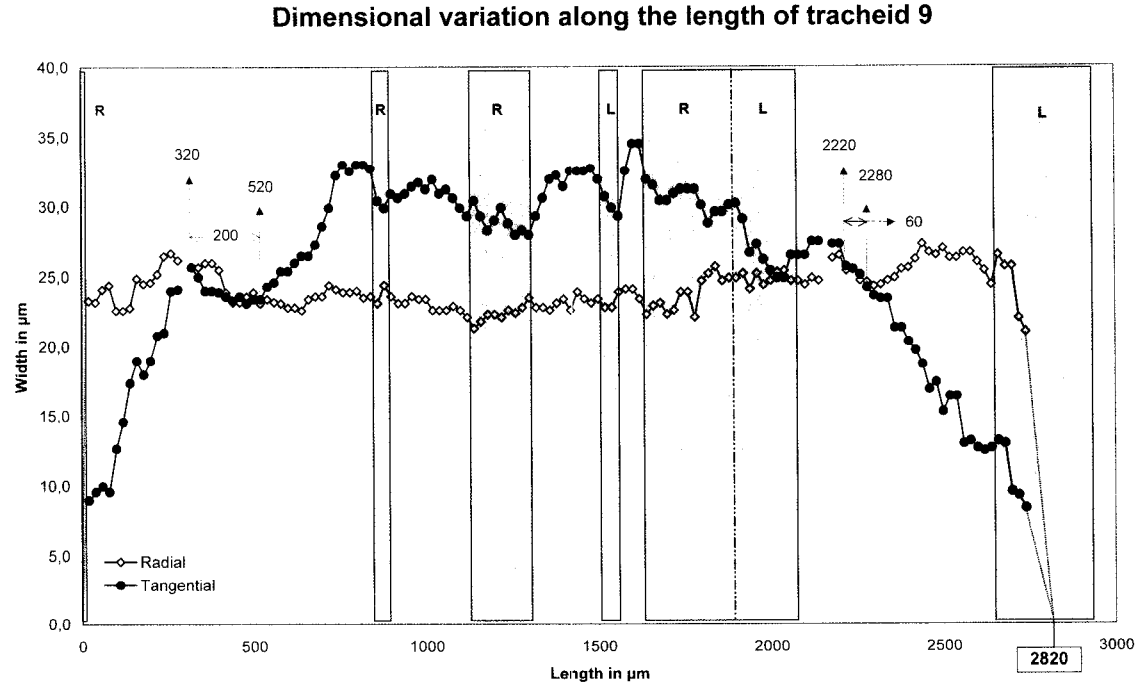
Dimensional variation along the length of tracheid 9
Width in µm
Length in µm
Radial
Tangential
R
L
320
520
200
2220
2280
60
2820
0,0
5,0
10,0
15,0
20,0
25,0
30,0
35,0
40,0
0
500
1000
1500
2000
2500
3000

FIG. 4.

TABLE 1. *Length of the tracheids studied. The shortest unit length corresponds to 20 μm.*

Tracheid no.	Length in μm						(Tip 1/Tip 2)
	Tip 1	T-zone 1	Middle zone	T-zone 2	Tip 2	Total length	
9	320	200	1700	60	540	2820	1.69
8	300	340	1680	20	500	2820	1.66
7	180	340	1940	20	380	2840	2.11
6	200	40	2220	20	380	2840	1.9
Average	250	230	1885	30	450	2830	1.84
ca.	9%	8%	67%	1%	16%	100%	

(version 4.0) and Rhinoceros (version 1.1). Mathematical and statistical calculations were performed with Microsoft Excel 97. The morphological variation within each tracheid transverse section was plotted along the total tracheid length. 3D reconstructions of tracheid segments were generated combining CAD (computer aided design) and visualization softwares. The images were aligned in relation to each other with the help of reference points (year ring border, rays, and neighboring tracheids). The transverse shape of tracheids was extracted from each image and positioned in sequence in the computer. 3D reconstruction was accomplished by separating the serial planes in the Z direction with a corresponding gap of 20 μm in between and linking the serial tracheid segment shapes using Non-Uniform Rational B-Splines (NURBS). Visualization was accomplished with a high degree of freedom, although here they are only displayed in tonalities of the grayscale. Although bordered and cross-field pits are of high importance in the study of tracheid microstructure, they were not displayed in the reconstructions presented in this work. A section thickness of 20 μm was necessary to get a complete set of transverse sections covering whole tracheids. This section thickness did not allow the detailed reconstruction of bordered and cross-field pits. Much thinner sections are needed to allow a more detailed 3D reconstruction of these structures.

RESULTS AND DISCUSSION

Tracheid morphology

Image analysis of serial micrographs revealed that the four latewood tracheids studied had a characteristic shape with alternating dimensions along the tracheid length. After plotting radial and tangential tracheid width along the tracheid length, it became evident that the tracheids were composed of distinct morphological zones (Figs. 1–4). Five different morphological zones were identified (Fig. 5). The lengths of these different zones are summarized in Table 1. At the beginning of the plots (Figs. 1–4), radial and tangential widths increase progressively, with the radial width exceeding the tangential width until a point where they coincide. This morphological zone was defined as the *first tracheid tip.* The length of this zone varied from 180 μm to 320 μm. Radial and tangential widths remain close with more or less the same value up to a certain length until they begin to delineate. This morphological zone was defined as the *first transition zone.* The length of this zone varied from 40 μm to 340 μm. After delineation, the tangential width increases, stabilizes, and decreases towards a second cross-over, while the radial width remains fairly constant and less than the tangential width. This third morphological zone was defined as the *middle zone.* The length of this zone varied from 1,680 μm to 2,220 μm. At the second cross-over, the radial wall width becomes greater than the tangential width. Here, the change in width dimension occurs more rapidly than at the *first transition zone.* This morphological zone was defined as the *second transition zone.* The length of the *second transition zone* varied from 20 μm (Figs. 1–3) to 60 μm (Fig. 4). Finally, the radial and tangential cell-wall width decreases, with the radial width exceed-

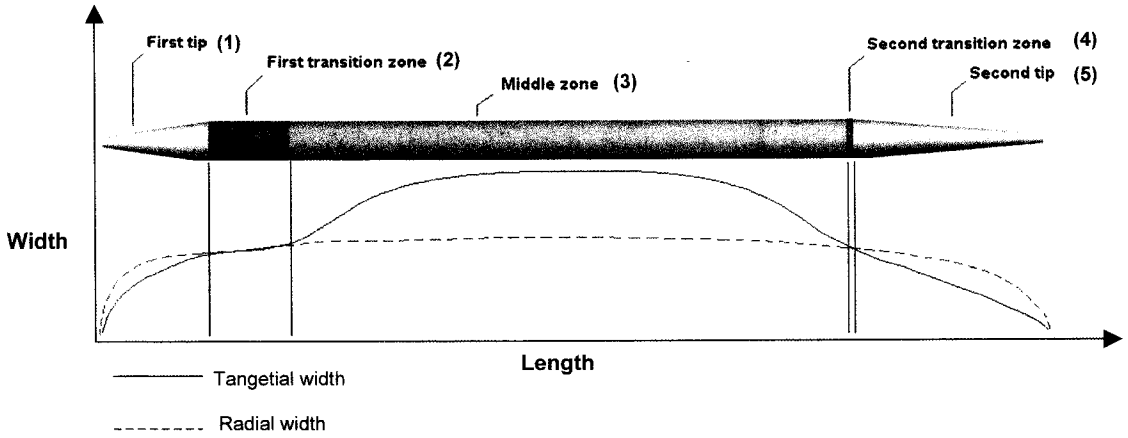

FIG. 5. Schematic representation of the 5 different tracheid morphological zones.

ing the tangential width until they coincide at the very tip of the tracheid. This last morphological zone was defined as the *second tracheid tip*. The length of this zone varied from 380 μm to 540 μm.

A closer examination of the plots revealed other interesting features. The tracheids studied were arranged radially in the same row with tracheid 6 closest to the annual ring border at the latewood side and tracheid 9 the most distant. Taking this into consideration, it is interesting to note that there is a change in dimension that seems to be closely related with the position of the tracheids in the row (Table 1). The length of the tracheid tips and transition zones showed a trend in becoming shorter towards the annual ring border. On the contrary, middle zones seem to become longer. A closer look at the dimensions of tracheid tips and transition zones revealed that the *first tracheid tips* are shorter than the *second tracheid tips*, and that on the contrary the *first transition zones* are larger than the *second transition zones* (Table 1, Figs. 1–4). This indicates that it should be possible to define the orientation of these tracheids in the stem with one tip pointing upwards and the other downwards. Unfortunately, this was not possible in this study. The data presented in Table 2 also show that the mean width dimensions as well as maximal width dimensions decrease towards the annual ring border. On the contrary, the tangential width at the point of maximal radial width increases towards the annual ring border. This implies that the *middle zone* morphology is also varying along the tracheid row.

Although tracheid width in Norway spruce has not been studied in such detail previously, some comparison with data by Fengel (1969) might be valid. In his work, the mean radial and tangential "diameters" of latewood tracheids are 13.1 and 32.1 μm, respectively. In the present study, the mean radial width of the tracheids studied varied from 17.8 μm to 25.9 μm, and the mean tangential width from 23.6

TABLE 2. *Radial and tangential widths along the tracheid length.*

	Radial width (μm)			Tangential width (μm)		
Tracheid no.	Mean	Max.	Tang. width at max.	Mean	max.	Rad. width at max.
9	24.1	27.3	18.7	25.4	34.5	24.1
8	25.9	29.9	28.9	26.4	35.3	26.3
7	20.2	24.6	30.3	24.8	32.5	19.2
6	17.8	20.5	31.7	23.6	31.7	20.5